Review Paper

Glass transition and instant freezing theories – A comparison of frozen-in temper stresses

Wolfgang Seifert, Andreas Maschke and Manfred Dubiel

Fachbereich Physik, Martin-Luther-Universität Halle-Wittenberg, Halle (Germany)

For many practical cases of tempering the temper stresses calculated by instant freezing theories are sufficient and in good agreement with experiments. The auhors give a brief summary of the theories by Adams and Williamson, Bartenev and Indenbom and discuss their numerical implementation. For example, frozen-in temper stresses are calculated and discussed within the model of a symmetrically cooled, infinite glass plate. Based on the numerical solution of the heat conduction equation with a given heat transfer coefficient, especially the influence of the initial temperature of quenching is investigated. Furthermore, a numerical algorithm is presented to calculate the temporal evolution of the permanent temper stresses for Indenbom's theory. Finally, as a practical example, residual stresses are determined in the surface of a tempered glass-particle composite system.

Glasübergang und Instant-Freezing-Theorien – Vergleich der eingefrorenen Wärmespannungen

Für viele praktische Anwendungsfälle des thermischen Vorspannens von Glas sind thermische Eigenspannungen, die auf der Grundlage von Instant-freezing-Modellen berechnet wurden, ausreichend und in guter Übereinstimmung mit dem Experiment. Die Autoren geben eine kurze Zusammenfassung der Instant-freezing-Modelle von Adams und Williamson, Bartenev sowie Indenbom und diskutieren ihre numerische Umsetzung. Als Beispiel werden eingefrorene Wärmespannungen im Rahmen des Modells einer symmetrisch abgekühlten, unendlich ausgedehnten Glasplatte endlicher Dicke berechnet und verglichen. Auf der Grundlage der numerischen Lösung der Wärmeleitungsgleichung bei vorgegebenem Wärmeübergangskoeffizienten wird insbesondere der Einfluß der Ausgangstemperatur der Abkühlung auf die Höhe der Spannungen diskutiert. Ferner wird ein numerischer Algorithmus präsentiert, um die zeitliche Ausprägung der thermischen Eigenspannungen für Indenboms Modell zu berechnen. Als praktisches Beispiel werden abschließend Eigenspannungen in der Oberfläche eines vorgespannten Glas-Teilchen-Verbundsystems bestimmt.

1. Introduction

The theory of the glass transition has a long history. During the last nearly 100 years a number of theoretical approaches has been developed to model the mechanical response of glass during cooling [1]. In the classic theory of annealing, Adams and Williamson [2] investigated slow cooling of glass plates in order to reduce stress generation. Typically, temperature in annealing is controlled to produce a constant cooling rate bringing about only small temperature equalization stresses. These are stresses evoked in a glass plate by the decay of a nearly parabolic temperature distribution existing in the plate after leaving the transformation range.

In tempering glass with cooling rates being much higher and varying with time, additional contributions to the final temper stresses have to be taken into account: these are solidification stresses and stresses of structural origin [1]. The latter arises even while glass is being cooled at a constant cooling rate [3].

Clearly, the structural or thermoviscoelastic theory is necessary for a deeper understanding of the nature of glass transition [4 and 5]. It is the only theory that refers to the "real" glass, but it requires a set of physical properties that may not be available in any case. Just then, instant freezing models using restricted operating parameters can also predict final temper stresses as well as the more sophisticated viscoelastic or structural theory.

In instant freezing theories the transformation range of glass is reduced to a single solidification temperature T_g. This simplification produces a discontinuity in the material behaviour at T_g: glass above T_g is treated as a stress-free fluid, while glass below T_g is regarded as an elastic solid without any stress relaxation. Nevertheless, for many practical cases of tempering, instant freezing theories yield sufficient results (see e.g. figure 1). This is due to the fact that temper stresses in glass quenched from relatively high temperatures are predominately temperature equalization stresses, i.e. the precise rheological properties of glass in the transformation range are of relatively little moment.

The present paper gives a brief summary of the theories by Adams and Williamson, Bartenev [6] and Indenbom [7]. For these theories, numerically calculated temper stresses are discussed and compared. Furthermore, the influence of the initial temperature of quenching and the temporal evolution of the temper stresses

Received 26 September 1997, revised manuscript 25 February 1998.

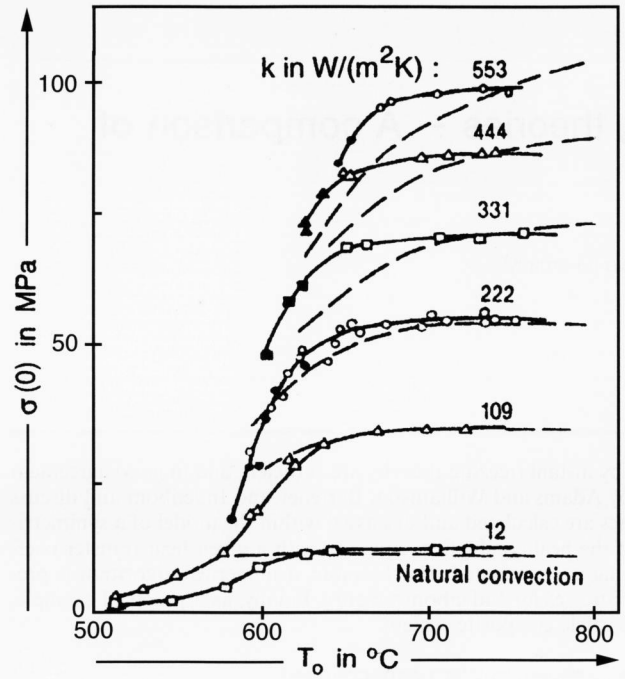

Figure 1. Influence of the initial temperature T_0 on the size of midplane stresses $\sigma(0)$ with heat transfer coefficient k as parameter [1, p. 154]: Experimental results and Bartenev's theory [6] (dashed lines).

Table 1. Processing parameters of the infinite glass plate model

density	ϱ	2.5 g/cm^3
specific heat	c_υ	775 J/(kg · K)
thermal conductivity	κ	0.87 W/(m · K)
linear thermal expansion coefficient	α	$8.9 \cdot 10^{-6}$ K^{-1}
elastic modulus	E	$6.98 \cdot 10^{10}$ Pa
Poisson's ratio	ν	0.247
glass transition temperature	T_g	575 °C
plate thickness	d	6.1 mm
initial temperature	T_0	635 °C
quenching temperature	T_1	26 °C
heat transfer coefficient	k	330.7 W/(m^2 · K)

(for Indenbom's theory) is investigated. Finally, as a practical example, the results are applied to determine residual stresses in the surface of a tempered glass-particle composite system. These systems are of specific interest in order to use their nonlinear optical properties [8]. All the following considerations are related to a flat glass plate that is large in relation to its thickness d:

$$-a \le x \le a,\ -b \le y \le b;\ -d/2 \le z \le d/2;\ a, b \gg d. \quad (1)$$

Both sides are symmetrically cooled with a given heat transfer coefficient k governing the rate of heat exchange between the glass (with the homogeneous initial temperature T_0) and the quenching medium (e.g. with room temperature T_1). For a region far from all edges the temperature distribution depends only on the z-coordinate and the heat conduction equation is one-dimensional

$$\varrho\, c_\upsilon \frac{T}{t} = \kappa \frac{^2T}{z^2}, \quad (2)$$

where $\varrho\, c_\upsilon$ is the volumetric specific heat and κ the thermal conductivity.

Within the model of an infinite glass plate the stresses produced are two-dimensionally isotropic plane stresses, varying through its thickness only:

$$\sigma_{xx} = \sigma_{yy} \equiv \sigma(z)\ ;\ \sigma_{zz} = 0\ . \quad (3)$$

Calculations were performed for a representative glass plate with the geometric and material parameters as shown in table 1.

Any theoretical description of tempering must start with a transient thermal conduction analysis, i.e. equation (2) has to be solved with initial and boundary conditions. For the case of tempering these are given by

$$T(z,0) = T_0 \text{ and } -\kappa\left(\frac{T}{n}\right)\Big|_{\pm d/2} = k(T - T_1)\Big|_{\pm d/2}\ . \quad (4)$$

The exact solution for this problem is given e.g. in [9] in the form of an infinite series which was used to calculate the temperature distribution $T(z,t)$ applying a sophisticated numerical technique with precalculated eigenvalues. This approach increases both precision and operation speed in comparison to numerical "standard methods" for solving partial differential equations of type (2).

Once the temperature distribution $T(z,t)$ is known, thermoelastic stresses can be calculated from first principles of thermoelasticity [10].

$$\sigma(z,t) = -2G\frac{1+\nu}{1-\nu}\alpha[T(z,t) - \overline{T(t)}]\ , \quad (5)$$

where G is the shear modulus and ν Poisson's ratio, α is the linear thermal expansion coefficient and $\overline{T(t)}$ the average temperature corresponding to the distribution $T(z,t)$. Note that these transient thermoelastic stresses are reversible. Also, for cooling, one gets tensile stresses in the surface being balanced by compression in the interior according to the required mechanical equilibrium of the glass plate:

$$\overline{\sigma(z,t)} = \frac{1}{d}\int_{-d/2}^{d/2} \sigma(z,t)\, \mathrm{d}z = 0\ . \quad (6)$$

The transient thermoelastic stresses (equation (5)) are the basis for evaluating permanent temper stresses within the framework of instant freezing theories. Instead of using a dynamical concept, all instant freezing

theories describe the glass transition from the standpoint of the static or quasi-static continuum mechanics and thermodynamics, respectively.

2. The model by Adams and Williamson

Adams and Williamson [2] investigated the annealing of glass as a process of removing or diminishing strains and corresponding internal stresses in glass by slow cooling at a constant cooling rate. In summary, the following two statements outline their qualitative model:

a) "The strain remaining in a block of glass is equal and opposite in sign to the ... strain lost by viscous yielding in the early stage of the cooling process" [2, p. 604].

b) "When a glass is heated to a relatively high temperature and then cooled at a constant rate, the final stress is exact the same as the temporary stress which would be caused by heating at the same rate" [2, p. 840].

Thus, temperature equalization stresses can be calculated from equation (5) by changing the sign and applying the temperature distribution at a time $t = t_g$:

$$\sigma^{AW}(z) = 2G\frac{1+\nu}{1-\nu}\alpha[T(z,t) - \bar{T}]_{t=t_g} . \tag{7}$$

In this model the glass transition is considered as a nonlocal process which occurs "at once" at the solidification time t_g. The time t_g can be computed e.g. by solving the equation

$$\frac{1}{d}\int_{-d/2}^{d/2} T(z, t = t_g)\,\mathrm{d}z = T_g . \tag{8}$$

Once the time t_g is known, the calculation of the permanent temper stresses (equation (7)) is easy.

The model by Adams and Williamson can be considered to be the simplest instant freezing model which holds also for tempering at moderate cooling rates even though the (predominating) temperature equalization stresses are not the only stresses brought forth.

For a plate of soda-lime-silica glass with a thickness $d = 6.1$ mm and properties given in table 1, some calculations are presented in figures 2 to 4.

Figure 2 shows temperature profiles across the whole plate at $t = t_g$ for several heat transfer coefficients k. As the initial temperature $T_0 = 635\,°C$ is distinctly above the solidification temperature ($T_g = 575\,°C$), there is enough time to build up a nearly parabolically shaped temperature profile even for relatively high quenching rates. Because of equation (7) this is also true for the corresponding stress profiles shown in figure 3.

The influence of the initial temperature T_0 on the magnitude of the final midplane stresses is shown in figure 4 for some heat transfer coefficients k already used in [1]. This allows a direct comparison of the results also shown in figure 1. Comparing figures 1 and 4, it becomes clear that the model by Adams and Williamson

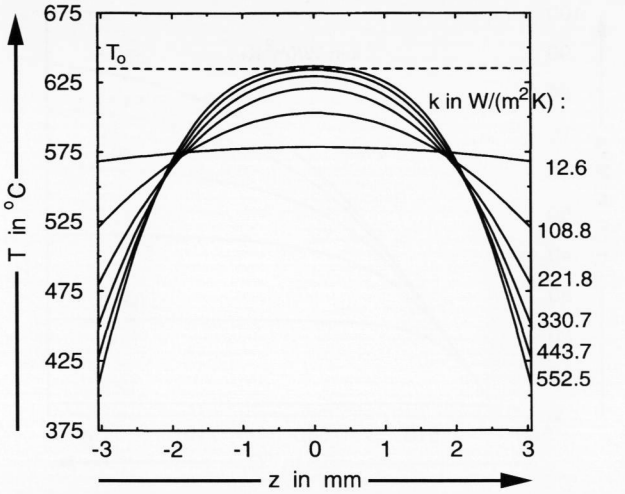

Figure 2. The model by Adams and Williamson [2]: Temperature at solidification across the whole plate.

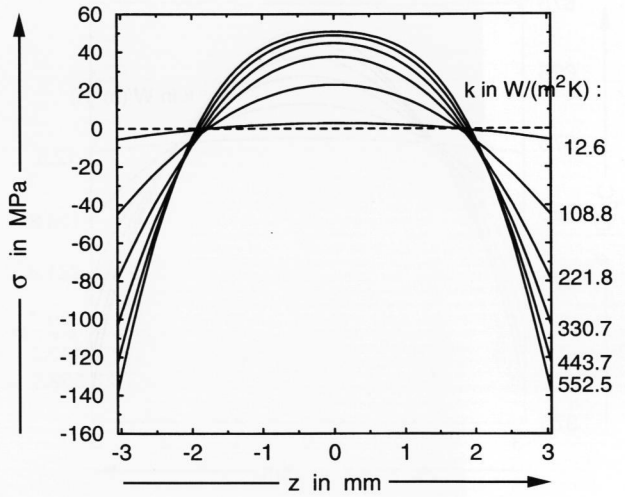

Figure 3. The model by Adams and Williamson [2]: Permanent stresses $\sigma(z)$ across the whole plate.

can only be a first approximation of the real behaviour. Especially, the influence of the initial temperature on the magnitude of the final temper stresses is too strong. The evident advantage of the model by Adams and Williamson is its simplicity. This makes it interesting for practical cases even today. In particular, it is very useful for estimating permanent temper stresses (for "regular conditions" of tempering) in glass specimens with real geometry by means of thermoelastic FEM calculations.

3. Bartenev's postulate

In 1949 Bartenev [6] proposed to treat glass as solidifying at a single transformation temperature T_g. Thus, the process of solidification is simply realized by travelling the T_g isotherme ("freezing front") from the surface to the midplane of the glass plate. Concerning the final temper stresses created after solidification by tempering,

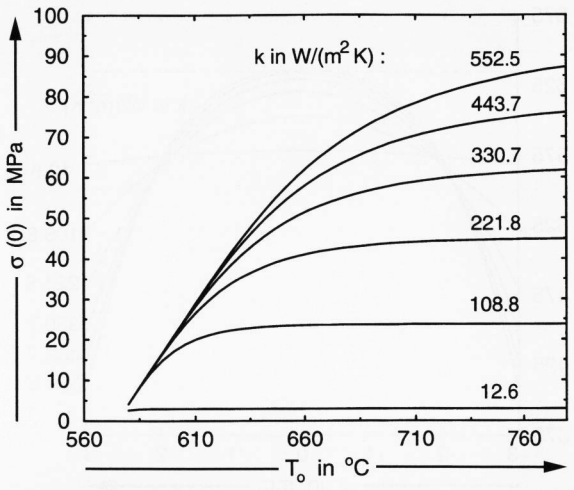

Figure 4. The model by Adams and Williamson [2]: Influence of the initial temperature T_0 on the size of midplane stresses $\sigma(0)$.

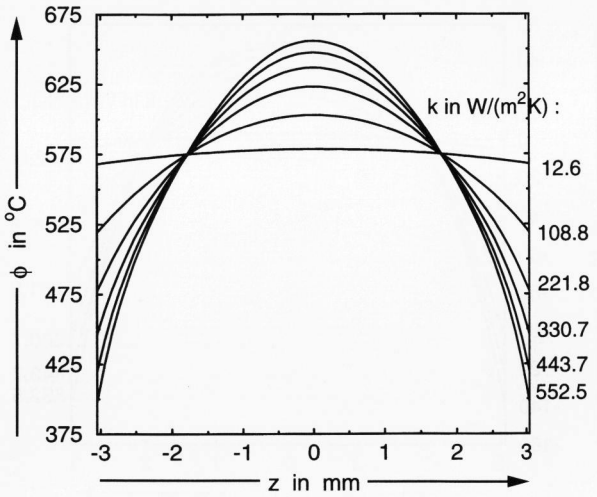

Figure 5. The model by Bartenev [6]: Fictitious temperature $\phi(z)$ across the whole plate.

Bartenev postulated to calculate them from the decay of a fictitious temperature distribution $\phi(z)$ defined by the equation

$$\frac{\mathrm{d}\phi}{\mathrm{d}z} = \left.\frac{\mathrm{d}T}{\mathrm{d}z}\right|_{T=T_g} . \tag{9}$$

This means that $\phi(z)$ results from the local temperature gradient calculated at the present position of the freezing front T_g. The numerical procedure for calculating $\phi(z)$ is straightforward: After computing the solidification time $t_g(z)$ for each position z inside the plate the right side of equation (9) is evaluated. In the second step equation (9) is integrated. Finally, the permanent temper stresses are calculated analogous to equation (7)

$$\sigma^{BV}(z) = 2G\frac{1+\nu}{1-\nu}\alpha[\phi(z) - \bar{\phi}] . \tag{10}$$

Bartenev's approach was the first that models the glass transition in a local manner by equation (9). As $\phi(z)$ differs from the temperature distribution $T(z)$, the final temper stresses (equation (10)) represent both the stresses brought forth during solidification and the temperature equalization stresses as a whole.

The critique of Bartenev's approach especially concerns the lack in the theoretical background. The model is inconsistent with the first principles of thermoelasticity and does not distinguish between stresses brough forth during solidification and temperature equalization stresses. In particular, this makes it impossible to calculate the temporal evolution of the permanent temper stresses. Nevertheless, Bartenev's theory holds for relatively high initial temperatures $T_1 \approx 650\,°C$ and moderately high quenching rates [1]. For the glass plate with properties given in table 1 the results are shown in figures 5 to 7.

The fictitious temperature profiles (figure 5) calculated from equation (9) obviously differ from the actual temperature distributions (figure 2). This affects the shape of the stress profiles (figure 6). But the magnitude of the stresses – especially the one of the interesting compressive stresses in the surface region – is nearly the same. This underlines the well-known fact, that temperature equalization stresses are predominant under "regular conditions" of tempering.

Finally, figure 7 presents the influence of the initial temperature on the final midplane stresses. At low temperatures near T_g no significant permanent stresses are built up because of the solidification occurring very early. With increasing T_0 stress relaxation comes into account resulting in permanent temper stresses with the opposite sign of the relaxed transient stresses. After reaching a temperature distinctly far above the transformation range no further increase of permanent stresses can be achieved because the solidification occurs when nearly all transient stresses have been relaxed to zero.

Note, that in spite of the quite different theoretical approaches, the models by Bartenev and by Adams and Williamson predict final temper stresses without significant differences for "regular conditions" of tempering (figures 4 and 7).

4. Indenbom's theory

Indenbom [7] was the first who succeeded in combining the first principles of thermoelasticity and the instant freezing theory to calculate permanent temper stresses. Rejecting Bartenev's work he intented to develop a consistent model without the need of any postulate. He recognized that, in addition to the elastic and the thermal part of strains, a further component of the total strain tensor has to be taken into account:

$$\tilde{\varepsilon}^{tot} = \tilde{\varepsilon}^{el} + \tilde{\varepsilon}^{th} + \tilde{\varepsilon}^{vis} . \tag{11}$$

The viscous strains $\tilde{\varepsilon}^{\mathrm{vis}}$ are known from hydrodynamics to describe viscous fluids; from a thermodynamical point of view, they may also contain contributions due to the dynamics of the glass transition, i.e. statistical hopping and cooperative motion of the glass atoms, respectively.

The elastic strains $\tilde{\varepsilon}^{\mathrm{el}}$ can be calculated if all other strains are known:

$$\tilde{\varepsilon}^{\mathrm{el}} \frac{1}{2} (\nabla \vec{u} + \vec{u} \nabla) - \alpha(T(z,t) - T_{\mathrm{ref}}) \tilde{E} - \tilde{\varepsilon}^{\mathrm{vis}} . \qquad (12)$$

$\tilde{E}$ denotes the unity tensor, ∇ is the nabla operator and $\vec{u}$ is the displacement vector. Note, that both the viscous strains and the thermal extra strains are of diagonal structure.

It is interesting to realize that no further assumptions are made about the viscous strains within Indenbom's theory; they may change as long as the considered part of the plate is fluid, i.e. has a temperature above T_{g}. Because only the frozen-in form of the viscous strains are important for the build-up of temper stresses, Indenbom denoted them separately as "residual strains" $\tilde{\varepsilon}^{\mathrm{res}}$:

$$\tilde{\varepsilon}^{\mathrm{res}} = \tilde{\varepsilon}^{\mathrm{vis}}|_{T=T_{\mathrm{g}}} . \qquad (13)$$

For the following considerations, the solidification of the glass is described by the progress of the freezing front Z in the upper half of the glass plate

$$T(t,Z) = T_{\mathrm{g}}, \quad Z = \frac{d}{2},\ldots,0 . \qquad (14)$$

Each position Z corresponds to a given solidification time $t_{\mathrm{g}}(Z)$ and vice versa.
Now, consider a time t_{g}^{0} where the freezing front Z is situated within the glass plate (figure 8). In this case the fluid and the solid parts of the plate have to be considered separately:

$$0 \le z < Z: \quad \tilde{\varepsilon}^{\mathrm{tot}} = \tilde{\varepsilon}^{\mathrm{th}} + \tilde{\varepsilon}^{\mathrm{vis}} , \qquad (15)$$

$$z = Z: \quad \tilde{\varepsilon}^{\mathrm{tot}} = \tilde{\varepsilon}^{\mathrm{th}} + \tilde{\varepsilon}^{\mathrm{res}} , \qquad (16)$$

$$Z < z \le \tfrac{d}{2}: \quad \tilde{\varepsilon}^{\mathrm{tot}} = \tilde{\varepsilon}^{\mathrm{el}} + + \tilde{\varepsilon}^{\mathrm{th}} + \tilde{\varepsilon}^{\mathrm{res}} . \qquad (17)$$

Note that in zones with $T \ge T_{\mathrm{g}}$ no elastic strains arise, i.e. the plate is stress-free for $0 \le z \le Z$. At the freezing front Z the following boundary condition holds for the total strains

$$\tilde{\varepsilon}^{\mathrm{tot}}|_{z=Z} = \tilde{\varepsilon}^{\mathrm{tot}}|_{z>Z} . \qquad (18)$$

No assumptions are made about the viscous (fluid) zone $z < Z$; in fact this is not necessary for the further considerations.

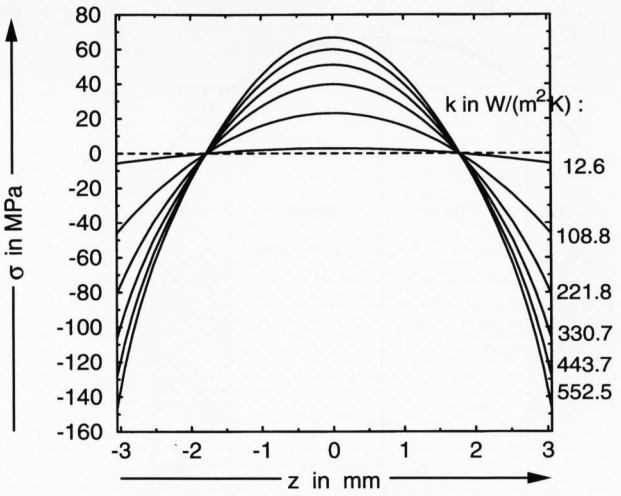

Figure 6. The model by Bartenev [6]: Permanent temper stresses $\sigma(z)$ across the whole plate.

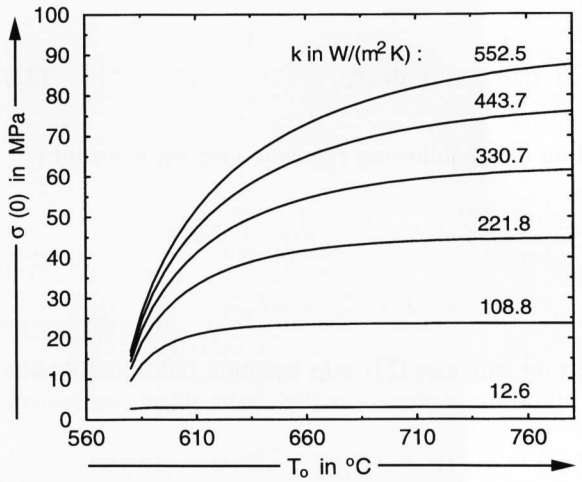

Figure 7. The model by Bartenev [6]: Influence of the initial temperature T_0 on the size of midplane stresses $\sigma(0)$.

Equations (11 and 13) can be considered as the basis of Indenbom's theory. Within the framework of the linear theory of elasticity he derived an expression which allows the calculation of transient as well as permanent temper stresses. To recall this, we presuppose the displacements u_x and u_y in the infinite plate to be given by

$$u_x = c_0 x , \quad u_y = c_0 y . \qquad (19)$$

Because of a constant total strain component $\varepsilon_{xx}^{\mathrm{tot}} = \dfrac{u_x}{x} = c_0$ one gets from equation (12) for the elastic strain component

$$\varepsilon_{xx}^{\mathrm{el}} = c_0 - \alpha(T(z) - T_{\mathrm{ref}}) - \varepsilon_{xx}^{\mathrm{res}} . \qquad (20)$$

The condition of mechanical equilibrium (equation (6)) concerns only the elastic zone

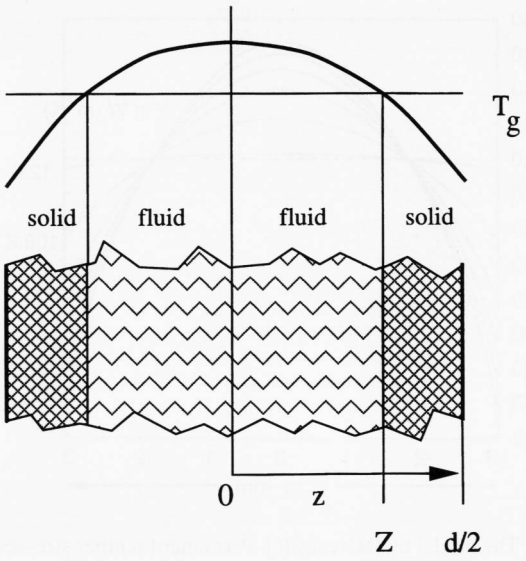

Figure 8. The model by Indenbom [7]: Definition of the freezing front Z.

$$0 = \int_{Z}^{d/2} \mathrm{d}z\, \sigma_{xx} = \int_{Z}^{d/2} \mathrm{d}z\, \varepsilon_{xx}^{\mathrm{el}}\,, \tag{21}$$

leading to the following expression for the constant c_0:

$$c_0 = \frac{\alpha}{\frac{d}{2} - Z} \int_{Z}^{d/2} \mathrm{d}z\, T(z) + \frac{1}{\frac{d}{2} - Z} \int_{Z}^{d/2} \mathrm{d}z\, \varepsilon_{xx}^{\mathrm{res}} - \alpha T_{\mathrm{ref}} \equiv \alpha \bar{T} + \overline{\varepsilon_{xx}^{\mathrm{res}}} - \alpha T_{\mathrm{ref}}\,. \tag{22}$$

Inserting equation (22) into equation (20), one obtains the following relations for the elastic strain component

$$\varepsilon_{xx}^{\mathrm{el}}(z,t) = \alpha[\bar{T}(t) - T(t,z)] + \overline{\varepsilon_{xx}^{\mathrm{res}}}(t) - \varepsilon_{xx}^{\mathrm{res}}(t,z)\,, \tag{23}$$

and for the transient temper stresses in the plate

$$\sigma^{\mathrm{IB}}(z,t) = 2G \frac{1+\nu}{1-\nu} \{\alpha[\bar{T}(t) - T(t,z)] + \overline{\varepsilon_{xx}^{\mathrm{res}}}(t) - \varepsilon_{xx}^{\mathrm{res}}(t,z)\}\,. \tag{24}$$

If the residual strains $\varepsilon_{xx}^{\mathrm{res}}$ are known, the temporal and spatial evolution of the stresses (equation (24)) can be calculated easily. This is the decisive advantage of Indenbom's model in comparison with the other models discussed before.

Since no high-speed digital computers were available at that time, Indenbom could only discuss special cases of equation (24) from a qualitative point of view. This concerns e.g. the final temper stresses which can be obtained from equation (24) taking the limit $t \to \infty$. In this case the temperature T is identical with its average $\bar{T}$ leading to

$$\sigma^{\mathrm{IB},\infty}(z) = 2G \frac{1+\nu}{1-\nu} [\overline{\varepsilon_{xx}^{\mathrm{res}}} - \varepsilon_{xx}^{\mathrm{res}}(z)]\,. \tag{25}$$

Besides, equation (24) also contains the purely elastic case: if glass is cooled down from temperatures $T < T_{\mathrm{g}}$, the material is primarily elastic with zero viscous strains leading to equation (5).

The essential problem is the numerical computation of the residual strains. To solve this problem, an integral equation will be derived next. It results from evaluating the boundary condition (18) for the total strain component $\varepsilon_{xx}^{\mathrm{tot}}$. Within the elastic zone $Z < z \leq d/2$ with equations (17 and 20)

$$\begin{aligned} \varepsilon_{xx}^{\mathrm{tot}} &= \varepsilon_{xx}^{\mathrm{el}}(z) + \varepsilon_{xx}^{\mathrm{th}}(z) + \varepsilon_{xx}^{\mathrm{res}} \\ &= \alpha[\bar{T} - T(z)] + \overline{\varepsilon_{xx}^{\mathrm{res}}} - \varepsilon_{xx}^{\mathrm{res}}(z) \\ &\quad + \alpha[T(z) - T_{\mathrm{ref}}] + \varepsilon_{xx}^{\mathrm{res}}(z) \\ &= \alpha[\bar{T} - T_{\mathrm{ref}}] + \overline{\varepsilon_{xx}^{\mathrm{res}}} \end{aligned} \tag{26}$$

is obtained.

At the freezing front, where the viscous strains are being frozen, this strain component is

$$\varepsilon_{xx}^{\mathrm{tot}} = \alpha[T(Z) - T_{\mathrm{ref}}] + \varepsilon^{\mathrm{res}}(Z) = \alpha[T_{\mathrm{g}} - T_{\mathrm{ref}}] + \varepsilon^{\mathrm{res}}(Z)\,. \tag{27}$$

By equating relations (26 and 27) to equation (18), finally

$$\overline{\varepsilon_{xx}^{\mathrm{res}}} - \varepsilon_{xx}^{\mathrm{res}}(Z) = \alpha(T_{\mathrm{g}} - \bar{T}) \tag{28}$$

is obtained. This expression represents an integral equation for the unknown quantities $\varepsilon_{xx}^{\mathrm{res}}(Z)$:

$$\frac{1}{\frac{d}{2} - Z(t)} \int_{Z(t)}^{d/2} \mathrm{d}z\, \varepsilon_{xx}^{\mathrm{res}}(z) - \varepsilon_{xx}^{\mathrm{res}}(Z(t),t) = \alpha \left[T_{\mathrm{g}} - \frac{1}{\frac{d}{2} - Z(t)} \int_{Z(t)}^{d/2} \mathrm{d}z\, T(z,t) \right]. \tag{29}$$

After solving equation (29) for each position $z = Z$ (corresponding to a solidification time $t_{\mathrm{g}}(Z)$) temper stresses can be evaluated easily using equation (24) or (25).

Equation (29) has been solved numerically on a fixed grid using sums instead of the integrals. To illustrate this, assume the z direction of the plate to be split into $2n$ intervals of equal length. Because of the symmetry only $n + 1$ points Z_{i} with $Z_0 = 0, \ldots, Z_n = d/2$ have to be considered. With the following definitions

$$E_i = \varepsilon_{xx}^{\mathrm{res}}(Z_i)\,, \tag{30}$$

$$T_i = \alpha(T_{\mathrm{g}} - \overline{T(Z_{\mathrm{i}})}) \tag{31}$$

equation (29) can be written in the following form:

$$\frac{1}{n+1-i} \sum_{j=i}^{n} E_j - E_i = T_i\,, \quad i = 0, \ldots, n\,. \tag{32}$$

This is a set of $n + 1$ equations for the $n + 1$ unknown values $E_0, \ldots, E_{\mathrm{n}}$. Taking into consideration equation (24)

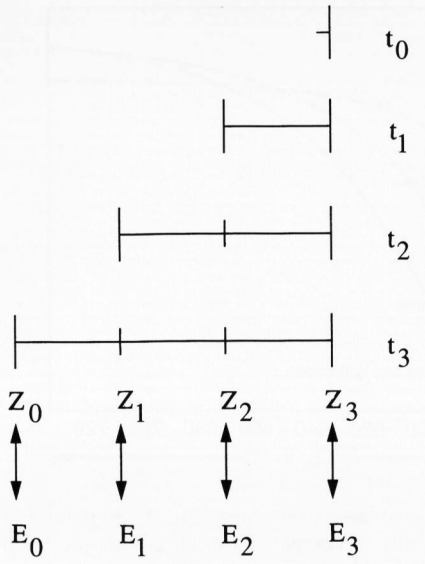

Figure 9. The model by Indenbom [7]: Visualization of the numerical algorithm.

the residual strains $\varepsilon_{xx}^{\mathrm{res}}(z)$ can be shifted by any constant. Choosing a value of $-\varepsilon_{xx}^{\mathrm{res}}(\frac{d}{2})$ one obtains the useful boundary condition

$$E_n = 0\,. \tag{33}$$

To demonstrate the algorithm, consider a grid consisting of only four points as shown in figure 9. In this case the following system of equations

$$\left.\begin{aligned} &\frac{E_0 + E_1 + E_2 + E_3}{4} - E_0 = T_0\,,\\ &\frac{E_1 + E_2 + E_3}{3} - E_1 = T_1\,,\\ &\frac{E_2 + E_3}{2} - E_2 = T_2\,,\\ &E_3 = T_3 = 0 \end{aligned}\right\} \tag{34}$$

has to be solved. This simple structure which also holds for the general case of n intervals

$$\left.\begin{aligned} &\frac{1}{n+1}\sum_{j=0}^{n} E_j - E_0 = T_0\,,\\ &\frac{1}{n+1-s}\sum_{j=s}^{n} E_j - E_s = T_s\,,\\ &-\frac{1}{2}E_{n-1} = T_{n-1} \end{aligned}\right\} \tag{35}$$

makes the solution very easy. The only non-trivial problem is the evaluation of T_i. This has been done by computing the solidification time for each (discrete) position z inside the glass plate:

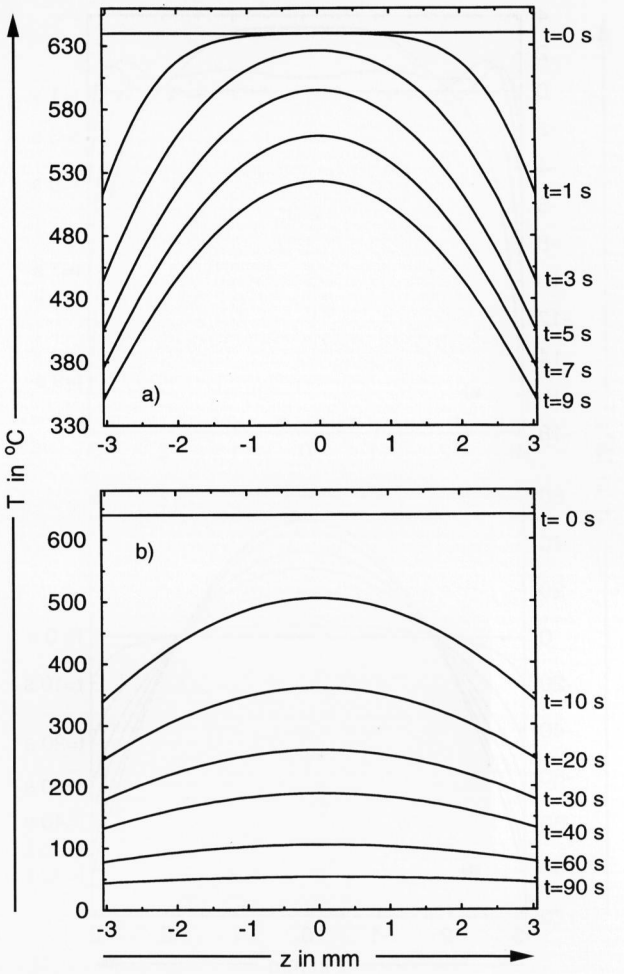

Figures 10a and b. The model by Indenbom [7]: Temporal evolution of temperature profiles $T(z)$ across the whole plate for a) $t < 10$ s, b) $t > 10$ s.

$$T_i = \alpha\left[T_{\mathrm{g}} - \frac{1}{n+1-i}\sum_{j=i}^{n} T(Z_j, t_i)\right]. \tag{36}$$

Applying this algorithm and using again the properties of the glass plate given in table 1, some results for Indenbom's theory will be presented next.

The temporal evolution of the temperature profile and the corresponding transient stresses are shown in figures 10a, b and 11a, b. Note that transient stresses in the glass plate during the first seconds of cooling (figure 11a) are quite small, only a few percent of the final temper stresses (figure 11b). Moreover, the stress distribution during the early stages of cooling shows a variety of different shapes including tensile stresses in the surface region. The latter, of course, strongly depends on both the initial temperature and the quenching rate.

In contrast to the models previously discussed, plateau levels of temper stresses already occur from initial temperatures of about 100 K above T_{g} (figure 12). Especially this result fits experimental data very well (see e.g. figure 1).

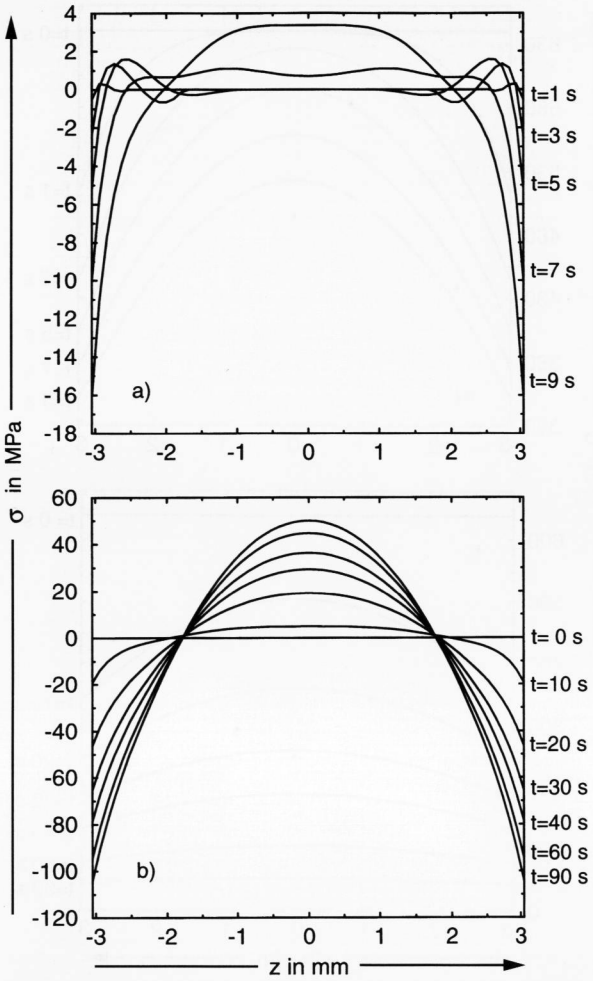

Figures 11a and b. The model by Indenbom [7]: Temporal evolution of frozen-in temper stresses $\sigma(z)$ across the whole plate for a) $t < 10$ s, b) $t > 10$ s.

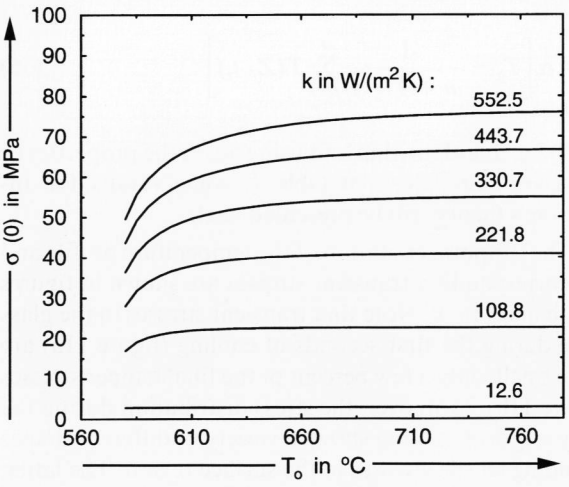

Figure 12. The model by Indenbom [7]: Influence of the initial temperature T_0 on the size of midplane stresses $\sigma(0)$.

A comparison of the three theories presented leads to the following results: For tempering with relatively low heat transfer coefficients, there is practically no difference

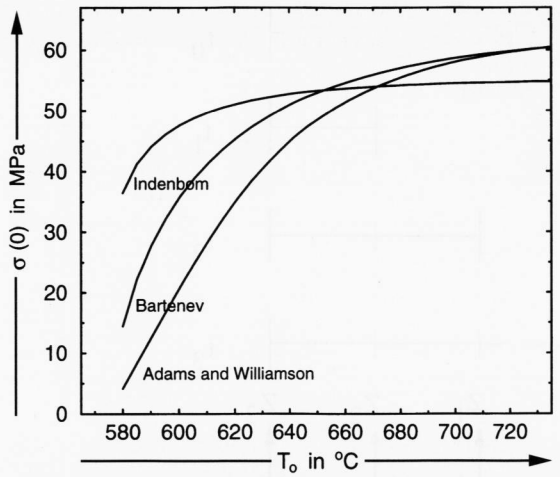

Figure 13. Influence of the initial temperature T_0 on the size of midplane stresses $\sigma(0)$: A comparison of all models presented (case $k = 330.7$ W/(m^2 · K)).

between the midplane stresses calculated. However, for higher quenching rates, Indenbom's theory predicts plateau levels of temper at lower temperatures than the theories by Bartenev and by Adams and Williamson (figure 13). This agrees with experimental data very well [1]. Significant differences occur for low initial temperatures near T_g and higher quenching rates. The reason for this is that the instant freezing assumption, neglecting the real transformation range of glass, is too rough.

5. *k*-fitting and application

In tempering the rate of heat exchange is primarily governed by the heat transfer coefficient k. It depends not only on the properties of both the tempering and the quenching medium but also on further processing conditions such as the surface state and the velocity of the quenching medium. Therefore, the heat transfer coefficient varies in a wide range. Usually, k is determined by measuring the time history curve of temperature $T(t)$ at the surface of the glass specimen and fitting a given analytical solution. To a first approximation, this can be done using the relation

$$T(t) = T_0 + (T_1 - T_0)\exp(-t/t_0) \tag{37}$$

with $t_0 = \dfrac{\varrho\, c_v\, d}{2k}$. Equation (37) turns out to be solution of the differential equation

$$\varrho\, c_v \frac{d}{2}\dot{T} = -k(T - T_0)\,, \tag{38}$$

which results from a balance of the thermal energy within the model of an infinite glass plate applying Newton's cooling law [11]. The unknown heat transfer coefficient k can be fitted e.g. by means of the computer algebra (CA) software MATHEMATICA.

Table 2. Permanent temper stresses of all models presented (quenching from $T_0 = 635\,°C$ to $T_1 = 26\,°C$): midplane tension $\sigma(0)$ and surface compression $\sigma(l)$, $l = \pm d/2$) for the theories by Adams and Williamson (A&W, equation (7)), Bartenev (BV, equation (10)) and Indenbom (IB, equation (25))

d in mm	theory	$k = 30$ W/(m² · K) $\sigma(0)$ in MPa	$\sigma(l)$ in MPa	$k = 100$ W/(m² · K) $\sigma(0)$ in MPa	$\sigma(l)$ in MPa	$k = 240$ W/(m² · K) $\sigma(0)$ in MPa	$\sigma(l)$ in MPa
0.2	A&W	0.19	−0.38	0.34	−0.68	0.24	−0.47
	BV	0.23	−0.45	0.76	−1.50	1.82	−3.60
	IB	0.23	−0.45	0.76	−1.50	1.81	−3.59
0.5	A&W	0.57	−1.12	1.47	−2.90	2.15	−4.23
	BV	0.57	−1.13	1.89	−3.75	4.51	−8.95
	IB	0.57	−1.13	1.89	−3.74	4.47	−8.90
1.0	A&W	1.20	−2.36	3.50	−6.90	6.52	−12.81
	BV	1.14	−2.25	3.76	−7.47	8.89	−17.76
	IB	1.14	−2.35	3.74	−7.43	8.73	−17.56
2.0	A&W	2.45	−4.83	7.58	−14.89	15.75	−30.76
	BV	2.27	−4.49	7.44	−14.84	17.13	−35.45
	IB	2.26	−4.48	7.33	−14.70	16.68	−33.97
4.0	A&W	4.30	−9.09	13.55	−28.45	29.28	−60.68
	BV	4.51	−8.95	14.49	−29.10	30.39	−61.66
	IB	4.46	−8.8	14.12	−28.67	30.24	−62.00
6.0	A&W	4.13	−11.25	13.10	−35.31	28.59	−75.69
	BV	6.71	−13.37	20.86	−42.00	40.20	−83.07
	IB	6.53	−13.07	20.37	−41.56	41.21	−85.18

A more precise result can be obtained by fitting the exact solution $T(d/2, t)$ of the heat conduction equation (2), with boundary conditions (equation (4)), to the measured time history curve of temperature $T(t)$ at the surface $z = \pm d/2$ of the glass plate. This solution was used to fit k applying a nonlinear Levenberg-Marquardt algorithm. In most practical cases the procedure converges very fast if the following initial or reference values for k are used:

- $k_{ref} = 30$ W/(m² · K), natural convection,
- $k_{ref} = 100$ W/(m² · K), forced convection (e.g. by a fan),
- $k_{ref} = 240$ W/(m² · K), symmetrical cooling in contact with metal plates.

For these k values representing typical situations of quenching [12], final temper stresses (i.e. midplane tension $\sigma(0)$ and surface compression $\sigma(l)$, $l = \pm d/2$ with plane structure (equation (3)) obtained from equations (7, 10 and 25)) have been calculated and listed in table 2 for all instant freezing theories considered. The stresses increase with both increasing k values and increasing thickness d of the glass plate. Note that relatively small differences occur for stresses calculated by different theories.

The authors have used these results to determine permanent temper stresses in the surface of a glass–particle composite system. Nanosized silver particles have been incorporated into the soda–lime–silica glass matrix by various methods, e.g. by ion implantation or by ion exchange followed by a thermal treatment or by electron irradiation [13]. Usually, the nanosized silver particles are formed in a surface layer of micrometre range [14]. In investigating such composite systems, the influence of the tempering process on their properties is of special interest.

For example, a specimen has been investigated with geometric parameters $a = b = 20$ mm, $d = 5$ mm. The time history curves of temperature $T(t)$ were measured by means of a thermocouple mounted on the surface of the glass plate by sodium trisilicate glass. The curves $T(t)$ and the results of the nonlinear Levenberg-Marquardt fitting are shown in figure 14 for the three quenching procedures mentioned above. Differences between the measured and the fitted curves are due to the fact that the model of an infinite glass plate does not completely reflect the experimental situation. Subsequently, the influence of both the specimen's finite volume (aspect ratio $a/d = 4$) and the thermocouple leads to a distribution of both temperature and stresses which is partially three-dimensional.

However, for valuable results to extract, the nonlinear fitting procedure uses a weighting function that guarantees a good agreement between the measured and the fitted time history curves for later times, while accepting differences in the first part of the curves.

Having fitted the heat transfer coefficient k, one can apply e.g. Indenbom's theory to calculate the final temper stresses (equation (25)) in the surface $z = l = \pm d/2$ of the specimen. The results are

for $k = 36$, 90, and 238 W/(m² · K),

$\sigma^{IB,\infty}(l) = -11$, -29, and -71 MPa,

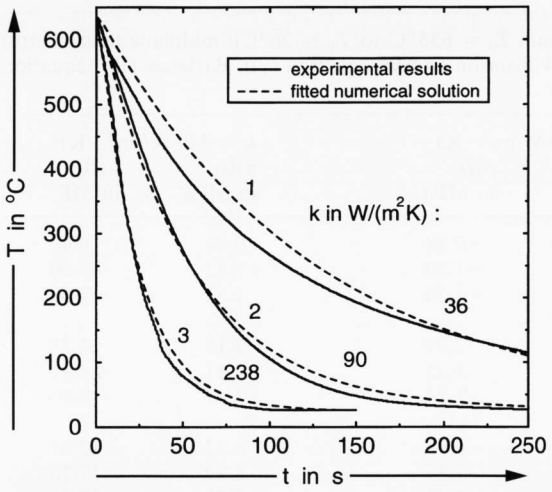

Figure 14. Measured and fitted time history curves of surface temperature $T(t)$ for a glass–particle composite system; quenching procedure from T_0 = 635 °C to T_1 = 26 °C by curves 1: natural convection, curves 2: forced convection, curves 3: contact with metal plates.

whereby the fitted k values sufficiently agree with the presumed reference values k_{ref} for the three quenching procedures used.

Thus, the cooling procedure of the specimen is not only connected with a thermoelastic effect on the nanosized particles [15]. Also, the build-up of a state of compression as a result of the tempering process should influence the structure and the properties of the nanosized silver particles as well. Investigations are in preparation in order to quantify these effects.

6. Conclusions

A brief review of instant freezing theories and their numerical implementation has been presented. For the theories by Adams and Williamson, Bartenev and Indenbom, frozen-in temper stresses have been calculated and discussed within the model of an infinite glass plate. All results have been calculated applying an interactive X11 program which has been developed to realize all numerical tasks from the fitting of experimentally measured time history curves of temperature up to the calculation of permanent temper stresses.

In comparison to the viscoelastic or structural theory, instant freezing theories require only a limited set of operating parameters. Moreover, they are quite easy to handle and can predict final temper stresses very well. To show this, a computer program was used to calculate permanent temper stresses in the surface of a tempered glass–particle composite system. Furthermore, this program enables to calculate residual stresses in any glass plates which have been strengthened by tempering.

Transient stresses in tempering can be calculated only by Indenbom's theory. For this theory, a numerical algorithm has been presented which allows the calculation of the temporal evolution of temper stresses. However, the instant freezing hypothesis leads to an underestimate of the transient surface tension [1]. As a consequence, transient stresses calculated from Indenbom's theory do not fit experimental data very well. This discrepancy can only be eliminated when the viscoelastic or the structural theory is applied with a proper description of the stress relaxation in the transformation range of glass [5 and 16].

7. Nomenclature

7.1 Symbols

a, b	length and width of the glass plate in mm
c_0	constant
c_v	specific heat in J/(kg · K)
d	thickness of the glass plate in mm
E	elastic modulus in Pa
$\tilde{E}$	unity tensor
G	shear modulus in Pa
k	heat transfer coefficient in W/(m² · K)
k_{ref}	reference value of k
$\vec{n}$	normal unity vector
t	time in s
t_g	solidification time in s
T	temperature in °C
T_g	glass transition temperature in °C
T_{ref}	reference temperature in °C
T_0, T_1	initial temperature in °C, quenching temperature in °C
$\vec{u}$	displacement vector in mm
x, y, z	cartesian coordinates in mm
Z	position of the freezing front in mm
α	linear thermal expansion coefficient in K^{-1}
$\tilde{\varepsilon}$	strain tensor
ϕ	fictitious temperature in °C
κ	thermal conductivity in W/(m · K)
ν	Poisson's ratio
ϱ	density in g/cm³
σ	stress in Pa
$\tilde{\sigma}$	stress tensor in Pa
∇	nabla operator

7.2 Superscripts

∞	limit $t \rightarrow \infty$
AW	Adams and Williamson
BV	Bartenev
IB	Indenbom
el	elastic
res	residual
th	thermal
tot	total
vis	viscous

*

The authors wish to thank Prof. Dr. S. Trimper, Martin-Luther-Universität Halle, and Dr. M. Schulz, Universität Ulm, for helpful discussions. This work was supported by the Deutsche Forschungsgemeinschaft (SFB 418), Bad Godesberg.

8. References

[1] Gardon, R.: Thermal tempering of glass. In: Uhlmann, D. R.; Kreidl, N. J. (eds.): Glass: Science and Technology. Vol. 5. New York (et al.): Academic Press, 1980. p. 145–217.

[2] Adams, L. H.; Williamson, E. D.: The annealing of glass. J. Franklin Inst. **190** (1920) p. 597–632, 835–870.
[3] Gardon, R.; Narayanaswamy, O.S.: Stress and volume relaxation in annealing flat glass. J. Am. Ceram. Soc. **53** (1970) p. 380–385.
[4] Ferry, J. D.: Viscoelastic properties of polymers. New York: Wiley, 1980.
[5] Mauch, F.; Jäckle, J.: Thermoviscoelastic theory of freezing of stress and strain in a symmetrically cooled infinite glass plate. J. Non-Cryst. Solids **170** (1994) p. 73–86.
[6] Bartenev, G. M.: Investigation of glass hardening. (Orig. Russ.) Zh. Tekh. Fiz. **19** (1949) p. 1423–1433.
[7] Indenbom, V. L.: On the theory of glass hardening (Orig. Russ.) Zh. Tekh. Fiz. **24** (1954) p. 925–928.
[8] Hache, F.; Ricard, D.; Flytzanis, C.: Optical nonlinearities of small metal particles: surface-mediated resonance and quantum size effects. J. Opt. Soc. Am. **B3** (1986) p. 1647–1655.
[9] Kneschke, A.: Differentialgleichungen und Randwertprobleme. Bd. 2. Leipzig: Teubner, 1961.
[10] Timoshenko, S. P.; Goodier, J. N.: Theory of Elasticity. New York: McGraw-Hill, 1970.
[11] Melan, E.; Parkus, H.: Wärmespannungen. Wien: Springer, 1953.
[12] Holman, L.P.: Heat transfer 3rd ed.. New York: McGraw-Hill, 1972.
[13] Hofmeister, H.; Thiel, S.; Dubiel, M. et al.: Synthesis of nanosized silver particles in ion-exchanged glass by electron beam irradiation. Appl. Phys. Lett. **70** (1997) no. 13, p. 1694–1696.
[14] Berg, K.-J.; Berger, A.; Hofmeister, H.: Small silver particles in glass surface layers produced by sodium-silver ion exchange – their concentration and size depth profile. Z. Phys. **D 20** (1991) p. 309–311.
[15] Miyata, N.; Jinno, H.: Strength and fracture surface energy of phase-separated glasses. J. Mater. Sci. **16** (1981) p. 2205–2217.
[16] Oel, H.J.; Helland, G.; Dannheim, H.: Thermisches Vorspannen von Glasscheiben. Glastech. Ber. **57** (1984) no. 1, p. 1–6.

1298P001

Address of the authors:

W. Seifert, A. Maschke, M. Dubiel
Fachbereich Physik
Martin-Luther-Universität
Halle-Wittenberg
Friedemann-Bach-Platz 6
D-06108 Halle